Published in final edited form as:
FEBS J. 2009 March ; 276(6): 1680–1697. doi:10.1111/j.1742-4658.2009.06900.x.

Inducible knockout mutagenesis reveals compensatory mechanisms elicited by constitutive BK channel deficiency in overactive murine bladder

Franz Sprossmann[1], **Patrick Pankert**[2], **Ulrike Sausbier**[1], **Angela Wirth**[3], **Xiao-Bo Zhou**[4], **Johannes Madlung**[2], **Hong Zhao**[1], **Iancu Bucurenciu**[1], **Andreas Jakob**[2], **Tobias Lamkemeyer**[2], **Winfried Neuhuber**[5], **Stefan Offermanns**[3], **Michael J. Shipston**[6], **Michael Korth**[4], **Alfred Nordheim**[2], **Peter Ruth**[1], and **Matthias Sausbier**[1]

[1]Pharmakologie und Toxikologie, Institut für Pharmazie, Universität Tübingen, Germany

[2]Proteom Centrum Tübingen, Interfakultäres Institut für Zellbiologie, Universität Tübingen, Germany

[3]Institut für Pharmakologie, Universität Heidelberg, Germany

[4]Institut für Pharmakologie für Pharmazeuten, Universitätsklinikum Hamburg-Eppendorf, Germany

[5]Institut für Anatomie, Universität Erlangen-Nürnberg, Germany

[6]Centre for Integrative Physiology, College of Medicine & Veterinary Medicine, University of Edinburgh, UK

Abstract

The large-conductance, voltage-dependent and Ca^{2+}-dependent K^+ (BK) channel links membrane depolarization and local increases in cytosolic free Ca^{2+} to hyperpolarizing K^+ outward currents, thereby controlling smooth muscle contractility. Constitutive deletion of the BK channel in mice ($BK^{-/-}$) leads to an overactive bladder associated with increased intravesical pressure and frequent micturition, which has been revealed to be a result of detrusor muscle hyperexcitability. Interestingly, time-dependent and smooth muscle-specific deletion of the BK channel (SM-$BK^{-/-}$) caused a more severe phenotype than displayed by constitutive $BK^{-/-}$ mice, suggesting that compensatory pathways are active in the latter. In detrusor muscle of $BK^{-/-}$ but not SM-$BK^{-/-}$ mice, we found reduced L-type Ca^{2+} current density and increased expression of cAMP kinase (protein kinase A; PKA), as compared with control mice. Increased expression of PKA in $BK^{-/-}$ mice was accompanied by enhanced β-adrenoceptor/cAMP-mediated suppression of contractions by isoproterenol. This effect was attenuated by about 60–70% in SM-$BK^{-/-}$ mice. However, the Rp isomer of adenosine-3′,5′-cyclic monophosphorothioate, a blocker of PKA, only partially inhibited enhanced cAMP signaling in $BK^{-/-}$ detrusor muscle, suggesting the existence of additional compensatory pathways. To this end, proteome analysis of $BK^{-/-}$ urinary bladder tissue was performed, and revealed additional compensatory regulated proteins. Thus, constitutive and

Correspondence P. Ruth, Pharmakologie und Toxikologie, Pharmazeutisches Institut, Universität Tübingen, Auf der Morgenstelle 8, D-72076 Tübingen, Germany. Fax: +49 7071 292476 ; Tel: +49 7071 2976781 peter.ruth@uni-tuebingen.de.

Europe PMC Funders Author Manuscripts

inducible deletion of BK channel activity unmasks compensatory mechanisms that are relevant for urinary bladder relaxation.

Keywords

cAMP/PKA signaling; overactive urinary bladder; proteomic adaptation; smooth muscle-specific BK channel knockout mice; time-dependent BK channel deletion

Europe PMC Funders Author Manuscripts

In mammals, the urinary bladder has two principal physiological functions, i.e. storage and voiding of urine. Urinary bladder voiding requires precise coordination of detrusor muscle contraction and concerted relaxation of internal and external urinary bladder sphincters. This process, which is under voluntary control in adults, involves a complex interplay of neuronal and smooth muscle-specific mechanisms, such as neurotransmitter release and intracellular Ca^{2+} signaling. Overactive bladder syndrome involves pathological myogenic and/or neuronal activities, often associated with increased detrusor muscle contractility [1–3]. There is strong *in vitro* and *in vivo* evidence that the large-conductance, voltage-dependent and Ca^{2+}-dependent potassium (BK) channel (synonyms: maxiK, $K_{Ca}1.1$, KCNMA1, Slo1) is an important regulator of urinary bladder smooth muscle (UBSM) contractility. This channel can limit Ca^{2+} entry through voltage-dependent Ca^{2+} channels by hyperpolarizing smooth muscle membrane potential and subsequently closing voltage-dependent Ca^{2+} channels [4–7]. The important contribution of BK channels to urinary bladder function was elucidated by using mice with a genetic deletion of the BK channel. Targeted deletion of the murine auxiliary smooth muscle-restricted β_1-subunit increases phasic contraction amplitude and frequency in the urinary bladder, but also reveals that BK channels – normally consisting of four pore-forming α-subunits and four accessory β_1-subunits in smooth muscle [8] – still contribute to the regulation of urinary bladder contractility [9], suggesting that BK channels formed by α-subunits alone can still be activated by Ca^{2+} and voltage in the urinary bladder. Genetic ablation of the pore-forming α-subunit, however, results in an overactive bladder associated with increased detrusor contractility, enhanced transmural bladder pressure, and increased micturition frequency [5,6]. Thus, the *in vitro* and *in vivo* characterization of BK channel knockout mice suggests a central role of the smooth muscle BK channel in regulating urinary bladder function. However, these findings cannot exclude the contribution of neuronal BK channels to urinary bladder function, as this channel type is ubiquitously expressed throughout the brain [10], parasympathetic nervous system [11], and dorsal root ganglia [12]. Thus, it is likely that the diverse functions of neuronal BK channels, e.g. repolarization of action potentials and generation of fast afterhyperpolarization, also contribute to the observed overactive bladder syndrome.

To address specifically the contribution of smooth muscle BK channels to the control of urinary bladder function, we established a conditional, temporally controlled smooth muscle-specific BK channel knockout (SM-$BK^{-/-}$) mouse line. The temporal control of this knockout model probably reduces potential compensatory mechanisms that may result in paradoxical phenotypes, as described recently in airway smooth muscle from mice with a constitutive deletion of BK channels ($BK^{-/-}$) [13]. Although treatment of the urinary bladder with the specific BK channel blocker iberiotoxin (IbTX) [6] should represent the

most straightforward ‘uncompensated’ state, this approach is limited by the low tissue penetration of the peptidergic toxin. Characterization of SM-BK$^{-/-}$ mice revealed an almost complete loss of BK channel protein expression in the urinary bladder within 1 week after induction. SM-BK$^{-/-}$ mice, which, unlike BK$^{-/-}$ mice, do not exhibit ataxia, showed a more severe overactive bladder phenotype than constitutive BK$^{-/-}$ mice. Comparative analysis of constitutive and conditional BK channel knockouts revealed functional compensation and proteomic adaptation in constitutive BK$^{-/-}$ mice masking – at least in part – the overactive bladder phenotype. Our conditional SM-BK$^{-/-}$ mouse line will help to determine the noncompensated contribution of smooth muscle BK channels to smooth muscle-restricted diseases.

Results

In wild-type littermate control of BK$^{-/-}$ (WT) murine urinary bladder, BK channel expression was restricted to the plasma membrane of detrusor muscle cells (Fig. 1A), and it was completely absent in the BK$^{-/-}$ urinary bladder (Fig. 1B). Analysis of BK channel expression in the SM-BK$^{-/-}$ urinary bladder revealed an almost complete loss of BK channel protein within 1 week after application of tamoxifen, which activates CreER^{T2}, leading to a conversion of the BK L2 allele to the knockout (L1) allele (Fig. 1C,D). BK channel positive staining in WT and wild-type littermate control of SM-BK$^{-/-}$ (Ctr) mice within the urothelium layer is restricted exclusively to vascular smooth muscle cells, as this staining disappears in the SM-BK$^{-/-}$ bladder (Fig. 1D). In non-smooth muscle tissues such as brain, no alteration of BK channel expression could be detected (Fig. 1E,F). Thus, evaluation of the BK channel expression profile in UBSM cells (UBSMCs) suggests a smooth muscle-specific knockout in the SM-BK$^{-/-}$ mouse line.

Membrane depolarization of UBSMCs from a holding potential of −10 mV elicited large noninactivating outward currents. The IbTX-sensitive component of the current, which represents the BK current (Fig. 2A,B, left), was completely absent in UBSMCs from mice lacking the BK channel α-subunit, whereas non-BK outward currents were not altered in these cells (Fig. 2A, right). In contrast, voltage-dependent Ca^{2+} current densities were significantly reduced in BK$^{-/-}$ but not SM-BK$^{-/-}$ UBSMCs when compared with WT mice, suggesting that downregulation of L-type Ca^{2+} channels compensates for constitutive BK channel deficiency (Fig. 2D). However, such a compensatory downregulation was not present when the BK channel was acutely deleted in SM-BK$^{-/-}$ mice, suggesting that adaptive processes during development may play a role in the reduction in L-type Ca^{2+} channel density. Furthermore, BK channel-deficient cells from BK$^{-/-}$ and SM-BK$^{-/-}$ mice exhibited a depolarized membrane potential of −25.8 ± 2.0 mV (BK$^{-/-}$) and −28.5 ± 1.7 mV (SM-BK$^{-/-}$) when compared to the corresponding controls (WT, −45.5 ± 3.8 mV; Ctr, −46.4 ± 2.1 mV), suggesting that BK channel activity contributes considerably to UBSMC membrane potential. A similar depolarization to that seen in BK-deficient UBSMCs was induced in WT and Ctr cells by the specific BK channel blocker IbTX (Fig. 2C), strengthening the hypothesis that BK channels are important dynamic regulators of UBSM membrane potential. As a functional consequence of this strong membrane depolarization, increased detrusor muscle contractility could be expected in BK knockout UBSMCs.

Apart from the important parasympathetic neurotransmitter acetylcholine, a variety of other neurotransmitters from efferent neural pathways as well as spontaneous myogenic activity, modulate detrusor muscle activity and thus micturition [14]. Neurotransmitter release and excitation of the urinary bladder during micturition was mimicked by electrical field stimulation (EFS) of the isolated organ (Fig. 3). EFS causes urinary bladder contractions, mainly by releasing neurotransmitters from nerve endings in the bladder body [15]. Increasing frequencies of EFS were applied to WT and mutant detrusor muscle strips with intact urothelium, and the initial peak of contraction was analyzed. Peak contractions were more accentuated and the maximal contraction was obtained at lower EFS frequencies in $BK^{-/-}$ and in SM-$BK^{-/-}$ detrusor muscle strips than in WT and Ctr mice. This effect was probably due to the more depolarized membrane potential of BK knockout detrusor muscle strips. However, there was also a striking difference in the contractile performance of $BK^{-/-}$ and SM-$BK^{-/-}$ detrusor muscle strips: peak contractions of SM-$BK^{-/-}$ strips were significantly stronger at 1, 2 and 4 Hz than in $BK^{-/-}$ strips. This difference in phenotype between the two BK channel knockout mouse lines points to reduced urinary bladder contractility having apparently developed in UBSM of mice with the constitutive deletion of BK channels. In order to exclude nonspecific effects of tamoxifen, EFS-induced detrusor muscle contractility was also determined in WT and $BK^{-/-}$ mice treated with the compound (Fig. S1). Tamoxifen had no significant effect on EFS-induced detrusor muscle contractility in WT or $BK^{-/-}$ mice.

To investigate the dynamic profile of detrusor muscle contractility, we analyzed the kinetic properties of EFS-induced contraction and spontaneous relaxation in urinary bladder strips from WT, Ctr, $BK^{-/-}$ and SM-$BK^{-/-}$ mice at frequencies of 4 and 30 Hz (Fig. 4). At the physiological frequency of 4 Hz [16], contractions elicited in SM-$BK^{-/-}$ urinary bladder strips were significantly stronger than in preparations from $BK^{-/-}$ mice, which developed an increased contractile force compared to WT and Ctr strips (Fig. 4). At the frequency of 30 Hz, detrusor muscle contractility was maximal (i.e. 100%) in all genotypes. At this frequency, $BK^{-/-}$ urinary bladder strips exhibited a significantly faster and more pronounced relaxation than SM-$BK^{-/-}$ strips. In contrast, contractions elicited in SM-$BK^{-/-}$ urinary bladder strips showed no alterations in relaxation kinetics when compared to WT or Ctr strips (Fig. 4). Notably, force development per tissue dry weight at maximal contraction was not significantly different between $BK^{-/-}$ (13.6 ± 1.7 $mN \cdot mg^{-1}$) and SM-$BK^{-/-}$ (14.4 ± 1.8 $mN \cdot mg^{-1}$) detrusor muscles. Again, tamoxifen had no influence on peak contraction and spontaneous relaxation in WT and $BK^{-/-}$ mice, excluding the possibility that tamoxifen treatment of Ctr and SM-$BK^{-/-}$ mice might have influenced the contractility of UBSM detrusor muscle strips. The different kinetic properties of detrusor muscle relaxation emphasize that temporally controlled BK channel deletion results in a more seriously increased detrusor muscle contractility than constitutive BK channel deletion.

The *in vivo* consequences of the increased $BK^{-/-}$ and SM-$BK^{-/-}$ detrusor muscle contractility in response to EFS were tested by long-term recordings of intramural pressure in awake, freely moving WT and $BK^{-/-}$ mice, using radiotelemetry. For intramural pressure analysis, the locomotor activity of the mice was taken into account. The distribution of the recorded intramural pressure revealed that values between 0 and 10 mmHg occurred less

frequently in $BK^{-/-}$ than in WT mice, whereas pressures above 10 mmHg occurred more often in $BK^{-/-}$ than in WT mice (Fig. 5A). This result suggests that increased contractility of detrusor muscle from $BK^{-/-}$ mice is reflected by an elevated urinary bladder tone in the mutants. A hallmark of elevated urinary bladder tone is an increased micturition frequency. To address this question, $BK^{-/-}$ mice, SM-$BK^{-/-}$ mice and the corresponding control mice were maintained without food and fluid for 5 h prior to a defined volume of water being given through oral tubing. For the following 3 h, the number of micturitions was recorded, and it was found to be increased 2.5-fold in $BK^{-/-}$ mice as compared with WT mice (WT, 1.4 ± 0.3; $BK^{-/-}$, 3.6 ± 0.5; Fig. 5B), indicating that the absence of the BK channel in UBSMCs results in an overactive urinary bladder and frequent micturitions. However, the micturition frequency in SM-$BK^{-/-}$ mice was substantially higher (~ eightfold) not only when compared to Ctr mice (SM-$BK^{-/-}$, 8.4 ± 1.9; Ctr, 1.0 ± 0.1), but also when compared to $BK^{-/-}$ mice (~ 2.3-fold). Tamoxifen as a control did not influence micturition frequency in WT and $BK^{-/-}$ mice (Fig. 5B). Taken together, these findings indicate that the overactive bladder phenotype is less prominent in $BK^{-/-}$ mice than in SM-$BK^{-/-}$ mice, again pointing to compensatory mechanisms becoming operative in constitutive knockouts.

Our findings so far suggest that the overactive urinary bladder of $BK^{-/-}$ mice reflects a hybrid phenotype resulting from gene deletion and subsequent long-term adaptation mechanisms rather than from the functional loss of BK channels alone. During the preparation of this article, Brown *et al.* 2008 [17] showed enhanced β-adrenoreceptor (β-AR) agonist isoproterenol (ISO)-mediated relaxations in $BK^{-/-}$ detrusor muscle precontracted by carbachol and KCl. Basically in agreement with their results, we observed enhanced suppression of EFS-induced contractions by ISO and the stable cAMP analog Sp-5, 6-dichloro-1-β-D-ribofuranosylbenzimidazole-3′,5′-monophosphorothioate (cBIMPS). To this end, detrusor muscle strips with intact urothelium were preincubated with either ISO (10 μM) (Fig. 6A–C) or cBIMPS (100 μM) (Fig. 6D) prior to EFS. ISO attenuated EFS-induced contraction in WT strips at 1, 2 and 4 Hz, but had no significant effect at 8 and 12 Hz. In contrast, EFS-induced contraction of $BK^{-/-}$ strips was significantly reduced by ISO at frequencies of 1, 2, 4, 8 and 12 Hz (Fig. 6B). In agreement with upregulation of cAMP signaling, ISO caused enhanced inhibition of $BK^{-/-}$ detrusor muscle contraction at 2, 4 and 8 Hz (13.2 ± 1.2%, 26.0 ± 1.2% and 27.5 ± 3.2% in $BK^{-/-}$ detrusor muscle; $n = 4$) when compared to WT detrusor muscle (4.4 ± 1.7%, 7.5 ± 1.6% and 11.0 ± 3.8%; $n = 4$) (Fig. 6C). This could be mimicked by the protein kinase A (cAMP kinase) (PKA) activator cBIMPS [18] at stimulation frequencies of 2, 4 and 8 Hz ($BK^{-/-}$, 13.7 ± 0.8%, 22.6 ± 0.9% and 20.4 ± 1.9% versus WT, 8.4 ± 1.8%, 9.1 ± 1.3% and 9.5 ± 3.7%; $n = 4$ per genotype) (Fig. 6D). Also EFS-induced detrusor muscle contractions were performed on SM-$BK^{-/-}$ and Ctr strips in the presence of ISO and cBIMPS (Fig. 6E,F). The agonists still inhibited contractions of SM-$BK^{-/-}$ detrusor muscle more efficiently than those of Ctr detrusor muscle, with significance at stimulation frequencies of 2 and 4 Hz. However, ISO (and likewise cBIMPS) increased the inhibition of SM-$BK^{-/-}$ contraction as compared to Ctr contraction only by 62% (2 Hz), 80% (4 Hz) and 36% (8 Hz), but by 200% (2 Hz), 246% (4 Hz) and 150% (8 Hz) in $BK^{-/-}$ detrusor muscle when compared to WT detrusor muscle (Fig. 6C,E). Here, it became apparent that Ctr and WT mice differ in their response to ISO (Fig. 6E,F versus Fig. 6C,D). This might be due to background differences (the Cre^{tg} C57Bl6 strain used for

generating SM-BK$^{-/-}$ mice differs from the C57Bl6 strain used for generating BK$^{-/-}$ mice; see also Experimental procedures) or the previous pharmacological treatment of the mice, i.e. application of tamoxifen to SM-BK$^{-/-}$ and Ctr mice, but not to BK$^{-/-}$ and WT mice. Nevertheless, the results suggest that the acute deletion of the BK channel in SM-BK$^{-/-}$ detrusor muscle attenuates the increased sensitivity of BK$^{-/-}$ detrusor muscle to ISO and cBIMPS. Moreover, upregulated cAMP signaling in the BK$^{-/-}$ urinary bladder may participate in the mitigated overactive bladder phenotype in BK$^{-/-}$ as compared to SM-BK$^{-/-}$ mice.

To evaluate the underlying compensatory mechanism, we focused on the expression of PKA, as β_3-adrenoceptor-mediated activation of this protein kinase is thought to inhibit urinary bladder activity [19–21]. Interestingly, we found significant increases in the expression of regulatory (1.92 ± 0.21-fold, n = 5 per genotype) and catalytic (1.53 ± 0.11-fold, n = 5 per genotype) subunits of PKA in the BK$^{-/-}$ urinary bladder when compared to the WT urinary bladder. In agreement with the increased PKA protein expression, the β-AR agonist ISO stimulated basal cAMP levels (WT, 0.61 ± 0.04 pmol·mg^{-1} wet weight; BK$^{-/-}$, 0.75 ± 0.05 pmol·mg^{-1} wet weight; n = 4 per genotype) 2.6-fold in the BK$^{-/-}$ urinary bladder (1.95 ± 0.51 pmol·mg^{-1} wet weight; n = 4) but only 1.3-fold in the WT urinary bladder (0.78 ± 0.02 pmol·mg^{-1} wet weight; n = 4) (Fig. 7B), suggesting that amplification of cAMP signaling proteins counterbalances the increased contractility in the BK$^{-/-}$ urinary bladder. Interestingly, the basal cAMP levels in the constitutive knockout urinary bladder were also significantly increased as compared to those in the WT urinary bladder (Fig. 7B). This could reflect protection of cAMP from degradation because of a higher level of expression of the PKA regulatory subunit. It should be noted that in the BK$^{-/-}$ urinary bladder we did not detect any alterations in the expression level of protein kinase G (cGMP kinase) (PKG) (BK$^{-/-}$, 99.2 ± 11.0%, as compared to WT; n = 6 per genotype) (Fig. 7A), which is also known to antagonize smooth muscle contraction. In contrast to what was found in the BK$^{-/-}$ urinary bladder, time-dependent deletion of smooth muscle BK channels (SM-BK$^{-/-}$) had no significant influence on protein expression levels of PKA (Fig. 7A).

To further elucidate the participation of PKA and its downstream effectors in detrusor muscle relaxation, we used the Rp isomer of adenosine-3′,5′-cyclic monophosphorothioate (Rp-cAMPS), a specific inhibitor of PKA. As PKA expression is upregulated in BK$^{-/-}$ detrusor muscle and ISO relaxes BK$^{-/-}$ detrusor muscle more efficiently than WT detrusor muscle, Rp-cAMPS, in the presence of ISO, should evoke stronger increases of EFS-induced contractions in BK$^{-/-}$ than in WT detrusor muscle. However, contractions of WT and BK$^{-/-}$ strips were only marginally increased by Rp-cAMPS/ISO versus ISO alone (Fig. 8), even though the increases caused by Rp-cAMPS were significant for BK$^{-/-}$ strips at frequencies of 2, 4 and 8 Hz. The latter observation suggests that only a minor part of the enhanced ISO-mediated relaxation of BK$^{-/-}$ detrusor muscle is based on upregulated PKA signaling (Fig. 7) and that the major part may involve other effectors of cAMP.

As only the minor part of the enhanced β-AR-mediated relaxation in BK$^{-/-}$ detrusor muscle could be inhibited by Rp-cAMPS and thus by PKA inhibition (Fig. 8), we were prompted to analyze the urinary bladder proteome using 2D SDS/PAGE combined with HPLC–ESI-MS/MS. The proteomic analysis revealed additional differentially expressed proteins, which

are summarized in Fig. 9. Interestingly, we found ~ 1.6-fold upregulation of smoothelin A (158 ± 8%; Fig. S3A), a marker protein of contractile smooth muscle cells [22] that is also upregulated in humans with overactive bladder syndrome [23].

Another example of an upregulated protein in the $BK^{-/-}$ urinary bladder is enolase 3 (216 ± 61% when compared to WT) (Fig. 9; Fig. S3B). Enolase 3, located at the sarcoplasmic reticulum (SR) as part of a glycolytic enzyme complex, is involved in local ATP synthesis by generating phosphoenolpyruvate [24,25]. A functional coupling between this enzyme complex and the sarcoendoplasmic reticulum-associated Ca^{2+}-ATPase (SERCA) has been shown. In fact, locally provided ATP rather than global ATP is essential for SERCA activity [26]. Thus, upregulation of enolase 3 in the $BK^{-/-}$ urinary bladder suggests enhanced synthesis of local ATP that subsequently results in higher SERCA activity, which in turn might increase Ca^{2+} uptake into the SR, thereby stimulating relaxation kinetics. Indeed, relaxation kinetics are enhanced in $BK^{-/-}$ detrusor muscle, as shown in Fig. 4. Further proteins that are substantially dysregulated in the $BK^{-/-}$ urinary bladder with putative roles in smooth muscle contraction and relaxation are presented in a proteome network (Fig. 10) (see Discussion).

Discussion

In this study, we exploited inducible, smooth muscle-specific loss of BK channel activity and found a more pronounced overactive urinary bladder syndrome manifested by increased micturition frequency and enhanced detrusor muscle contractions as compared with the constitutive BK channel knockout. These phenotypic results could be traced back to compensatory mechanisms being operative in the constitutive knockout detrusor muscle. As an underlying compensatory mechanism in $BK^{-/-}$ detrusor muscle, we identified a reduced L-type Ca^{2+} current density that was not present in the urinary bladder from mice with acute ablation of the BK channel. In agreement with Brown *et al.* [17], cAMP signaling was enhanced, with contractions of detrusor muscle being more efficiently relaxed by β-AR agonists and cAMP in $BK^{-/-}$ mice (Fig. 6). This was reflected by upregulation of catalytic as well as regulatory subunits of PKA (Fig. 7). The enhanced β-adrenergic/cAMP signaling was attenuated (Fig. 6E versus 6C) or even abolished (Fig. 7) after acute tamoxifen-triggered deletion of urinary bladder BK channels. Petkov *et al.* [27] and Hristov *et al.* [28] suggested that stimulation of β-AR in UBSMCs results in PKA-mediated activation of Ca^{2+} pumps and ryanodine receptors (RyRs), which generate Ca^{2+} sparks, leading to activation of the BK channel. However, loss of BK channels activates β-adrenergic signaling pathways independently of BK channels. These mechanisms are apparently upregulated in $BK^{-/-}$ detrusor muscle, and overcompensate for the loss of the BK channel in β-adrenergic signaling (Fig. 6). Moreover, the minor effect of Rp-cAMPS in inhibiting enhanced β-adrenergic signaling in $BK^{-/-}$ detrusor muscle suggests that even PKA-independent pathways [29] are implicated in ISO-induced relaxation of $BK^{-/-}$ detrusor muscle (Fig. 8). To identify putative proteins that may be regulated in $BK^{-/-}$ mice additionally to the L-type Ca^{2+} channel and PKA, a proteomic analysis was performed, and revealed further candidates such as calponin, enolase and smoothelin, which may also contribute to the maintenance of reasonable function of the urinary bladder and prevent a dramatic increase in micturition frequency in $BK^{-/-}$ mice.

The *in vitro* and *in vivo* characterization of the constitutive BK channel knockout model by Meredith *et al.* [5] and Thorneloe *et al.* [6] points to the central role of the smooth muscle BK channel in the regulation of urinary bladder function. However, the findings in this constitutive BK channel knockout model do not exclude the contribution of neuronal BK channels in urinary bladder function, as this channel type is ubiquitously expressed throughout the brain [10], spinal cord [11], and dorsal root ganglia [12]. These neuronal compartments are involved in the regulation of urinary bladder function [30]. Thus, it seems plausible that neuronal BK channels, which participate in repolarization of action potentials and generate fast after hyperpolarization, may contribute to the observed overactive bladder syndrome in constitutive BK channel knockout mice. In the present study, we established a smooth muscle-specific BK channel knockout mouse model in which the targeted deletion of the channel is temporally controlled and allows the acute deletion of smooth muscle BK channels. This permits analysis of the independent phenotype of UBSM BK channel deficiency while minimizing compensatory mechanisms accumulating over time after constitutive deletion of BK channels, which may partially mask the contribution of smooth muscle BK channels to urinary bladder relaxation. The inducible tissue-specific mouse model results in very efficient depletion of smooth muscle BK channels 1 week after tamoxifen application.

BK channels regulate membrane potential in detrusor muscle, as reported in arterial and tracheal smooth muscle [13,31]. In smooth muscle, BK channels are supposed to couple functionally to L-type Ca^{2+} channels via a negative feedback loop. Smooth muscle-specific deletion of L-type Ca^{2+} channels results in detrusor muscle quiescence and in urinary bladder atony [32], contrasting with the overactive bladder syndrome in smooth muscle-specific $BK^{-/-}$ mice. The more depolarized membrane potential in $BK^{-/-}$ detrusor muscle cells may result in incomplete inactivation of previously opened L-type Ca^{2+} channels. The resulting ‘window current’ [33] may increase Ca^{2+} influx and force development, although the density of the L-type Ca^{2+} channels appeared to be downregulated (Fig. 2D).

What can we learn from the functional characterization of tissue-specific $BK^{-/-}$ mice with regard to overactive bladder syndrome? The functional characterization and proteomic analysis of $BK^{-/-}$ mice suggest that the organism is challenged by loss of the BK channel and responds with compensation to maintain a certain level of physiological urinary bladder function. Although occurring to a smaller extent than in $BK^{-/-}$ mice, compensatory changes also seem to emerge in the inducible, smooth muscle-specific $BK^{-/-}$ mice (Fig. 6E,F), suggesting a reactive rather than a developmental adaptation to these changes. Nevertheless, constitutive $BK^{-/-}$ mice displayed an overactive bladder syndrome, demonstrating that the important role of BK channels in detrusor muscle function cannot be fully substituted for by enhancing the activity of other pathways involved in UBSM relaxation. This contrasts with observations from airway smooth muscle, where compensatory upregulation involving cGMP signaling in $BK^{-/-}$ mice apparently switches the expected phenotype from hypercontractility to hypocontractility [13].

What further insights into the pathophysiology of overactive bladder syndrome are provided by proteome analysis of the $BK^{-/-}$ urinary bladder? Constitutive deletion of the BK channel results in compensatory upregulation of the cAMP/PKA pathway, which is thought to

mediate sympathetic-induced relaxation of detrusor muscle. As blockage of PKA by Rp-cAMPS was insufficient to reverse the enhanced ISO-mediated inhibition of contraction, cAMP pathways other than PKA may be involved [29]. Another finding is the increased expression of the actin-binding protein smoothelin A – a contractile visceral smooth muscle marker [34] – in the $BK^{-/-}$ urinary bladder, which might be functionally relevant for the observed $BK^{-/-}$ urinary bladder phenotype. Targeted deletion of smoothelin A in mice revealed an essential role of this protein in smooth muscle contractility: smoothelin A knockout mice display a fragile gastrointestinal tract with strongly reduced intestinal contractility [35]. Thus, the upregulation of smoothelin A should promote hypercontractility of the $BK^{-/-}$ urinary bladder. Speculatively, upregulation of smoothelin A may be the consequence of increased Ca^{2+}-dependent transcriptional activity at the smoothelin gene locus. Increased smoothelin A expression was also found in humans with overactive bladder syndrome [23], suggesting that dysfunctions in bladder contractility converge at specific regulatory proteins.

Substantially dysregulated proteins of the $BK^{-/-}$ urinary bladder were integrated into a proteome network, illustrated in Fig. 10. Calponin (upregulated in proteomics; Fig. 9) inhibits the actin-activated Mg^{2+}- ATPase activity of myosin and maintains cells with unphosphorylated myosin in a relaxed state [36]. Glutathione *S*-transferase, including the omega 1 isoform (downregulated in proteomics; Fig. 9), has been found to differentially modulate the activity of the RyR1 and RyR2 calcium channel types [37].

A ubiquitously expressed protein is Ca^{2+}-dependent tissue transglutaminase (TG2, downregulated in proteomics; Fig. 9), which crosslinks glutamate and lysine residues intracellularly and in extracellular matrix organizations [38,39]. In addition, cell surface TG2 plays a role in cell adhesion and migration by binding to integrins [40]. Furthermore, TG2 can switch between a Ca^{2+}-bound and a GTP-bound state. The GTP-bound form is characterized as Ghα protein, which acts as a G-protein, functionally coupled to α_{1B} [41] and α_{1D} adrenoceptors [42], and regulates BK channel activity [43]. Activation of $\alpha_{1B/1D}$ adrenoceptors stimulates GDP–GTP exchange of TG2/Ghα, thus activating phospholipase Cδ1 and resulting in an increase of $[Ca^{2+}]_i$ [44,45]. In rabbit urinary bladder, α_1-adrenoceptors were reported to determine smooth muscle tone predominantly in the dorsal bladder and bladder neck [46,47]. Thus, TG2/Ghα downregulation might reduce $\alpha_{1B/1D}$-adrenoceptor-mediated contractions and muscle tone.

The suggested network reflects only a small aspect of potential compensatory protein regulation, as only soluble proteins, and not highly hydrophobic membrane-integrated ion channels, ion pumps, G-protein-coupled receptors or low-abundance signaling proteins such as kinases, can be reliably analyzed by 2D gel electrophoresis and HPLC–ESI-MS/MS. Furthermore, the experimental proof-of-concept of the differentially expressed proteins, found by 2D gel electrophoresis, and thus of their corresponding signaling pathways is missing, owing to the limitations of commercially available specific antibodies as well as the lack of specific pharmacological blockers for experimental verification of the proteome data.

What are the implications for future overactive bladder syndrome treatments? Besides the commonly used antimuscarinergic drugs [1,2,48], β_3-adrenoceptor agonists [49] emerge as

new therapeutics. The compensatory upregulated cAMP pathway in $BK^{-/-}$ mice reflects the importance of this signaling pathway as a possible rescue mechanism in overactive bladder syndrome. BK channels are essential for normal urinary bladder function, so BK channel openers/activators are also taken into consideration as therapeutics [50,51], despite the risk of seizures when they permeate the brain–blood barrier [52]. Also, gene therapy represents a putative clinical approach for overactive bladder syndrome treatment. Injection of BK channel DNA ameliorates detrusor muscle hyperactivity [53].

Experimental procedures

Constitutive and conditional BK knockout mice

$BK^{-/-}$ male mice WT mice (at an age of 3–4 months) were produced on an SV129 × C57Bl6 hybrid background (F2 generation) as previously described [54]. To establish the SM-$BK^{-/-}$ mouse line, mice with *loxP*-flanked alleles (BK L2/L2; SV129 background) of the BK gene *KCNMA1* [54] were intercrossed with transgenic mice expressing the tamoxifen-dependent Cre recombinase $CreER^{T2}$ under control of the smooth muscle-specific myosin heavy chain (SMMHC) gene *Myh11*. The generation of this SMMHC$CreER^{T2}$ mouse line (C57BL6 background) is described in detail by Wirth *et al.* [55]. Progenies both carrying two BK L2 alleles and transgenic for SMMHC-$CreER^{T2}$ were then crossed with BKL1/+ (SV129 background) mice to obtain SMMHC-$CreER^{T2}$ transgenic BKL2/L1 (SM-$BK^{-/-}$) and BKL2/+ (Ctr) mice. The correct genotype was analyzed by PCR amplification as described previously [54,55]. An intraperitoneal application of tamoxifen at 8 weeks of age (1 mg per day for five consecutive days) results in conversion of the *loxP*-flanked BK allele (L2) into a BK knockout allele (L1) specifically in smooth muscle. Either litter-matched or age-matched male mice (at an age of 3–4 months) with a hybrid SV129/C57BL6 background (always F2 generation) were randomly assigned to the experimental procedures with respect to the German legislation on animal protection.

Immunohistochemistry of the urinary bladder

On-slide 12 μm cryostat slices from nonfixed murine urinary bladder were preincubated with 10% normal donkey serum in buffer (1% BSA/0.5% Triton X-100/0.05 M NaCl/Tris). After being rinsed with NaCl/Tris, the slices were incubated with anti-BKα(674–1115) [10] (1 : 1000 in buffer) and tagged with an Alexa 555-conjugated donkey anti-(rabbit IgG) (1 : 1000 in buffer). BK expression was analyzed using a confocal-laser scanning microscope (Biorad MRC1000 attached to a Nikon Diaphot 300 equipped with a krypton–argon laser).

Electrophysiological recordings of UBSMCs

The urinary bladder was dissected and cut into small pieces prior to digestion at 37 °C for 30 min in Ca^{2+}-free physiological saline solution (PSS) (130 mM NaCl, 5.9 mM KCl, 2.4 mM $CaCl_2$, 1.2 mM $MgCl_2$, 11 mM glucose, 10 mM Hepes, pH 7.4) containing 0.7 $mg \cdot mL^{-1}$ papain, 1 $mg \cdot mL^{-1}$ dithiothreitol, and 1 $mg \cdot mL^{-1}$ BSA. The buffer was exchanged for PSS (containing 0.05 mM Ca^{2+}, 1 $mg \cdot mL^{-1}$ collagenase type H, 1 $mg \cdot mL^{-1}$ hyaluronidase, 1 $mg \cdot mL^{-1}$ BSA), and the tissue pieces were digested for a further 15 min at 37 °C. The remaining tissue was transferred to PSS and triturated to yield single UBSMCs. The cell dispersion was kept at room temperature until electrophysiological measurements were

performed. For recording membrane currents (whole cell mode), the bath solution was PSS, the pipette solution contained 136 mM KCl, 6 mM NaCl, 1.2 mM $MgCl_2$, 5 mM EGTA, 11 mM glucose, 3 mM dipotassium-ATP and 10 mM Hepes (pH 7.4), and the free Ca^{2+} concentration was adjusted to 300 nM. The holding potential was −10 mV, and test pulses of 300 ms duration were applied every 5 s to potentials ranging from −60 to +80 mV.

For measuring membrane potentials (using the nystatin-perforated patch configuration), the bath solution was PSS, and the pipette solution contained 110 mM potassium aspartate, 30 mM KCl, 10 mM NaCl, 1 mM $MgCl_2$, 0.05 mM EGTA, 10 mM Hepes (pH 7.2), and 250 $\mu g \cdot mL^{-1}$ nystatin. For recording voltage-dependent Ca^{2+} currents in the whole cell configuration, the pipette solution contained 110 mM CsCl, 20 mM tetraethylammonium (TEA^+), 2 mM $MgCl_2$, 10 mM EGTA, 5 mM ATP, 10 mM Hepes, and 10 mM glucose, adjusted to pH 7.2 with CsOH. The bath solution contained 10 mM $BaCl_2$, 130 mM TEA^+, 2 mM $MgCl_2$, 10 mM Hepes, and 10 mM glucose, adjusted to pH 7.2 with TEA-OH. UBSMCs were voltage-clamped at a holding potential of −60 mV, and the potential was increased stepwise for 300 ms every 5 s in 10 mV increments up to +50 mV. The inward current was measured as peak inward current with reference to zero current. A low-pass filter was set at a cut-off frequency of 1 kHz, and signals were digitized at 5 kHz. Data acquisition and analysis were performed with an ISO-3 multitasking patch-clamp program (MFK, Niedernhausen, Germany).

In vitro analysis of detrusor muscle contractility

Dissected urinary bladder was placed in ice-cold dissection solution (containing 80 mM monosodium glutamate, 55 mM NaCl, 6 mM KCl, 10 mM glucose, 2 mM $MgCl_2$, and 10 mM Hepes, pH 7.3), and opened longitudinally prior to segmenting the detrusor muscle into four muscle strips (each 2 × 4 mm). Muscle strips were mounted in organ baths (TSZ-04; volume 5 mL; Experimetria Ltd, Budapest, Hungary) that were filled with buffer (37 °C) containing 119 mM NaCl, 4.7 mM KCl, 1.2 mM KH_2PO_4, 2.5 mM $CaCl_2$, 1.2 mM $MgSO_4$, 11 mM glucose, and 24 mM $NaHCO_3$, aerated with 5% CO_2 in O_2 (pH 7.4). The muscle strips were equilibrated at 3 mN resting tension for 90 min, with buffer exchanges every 10 min. Tension was recorded isometrically. Contractions were provoked by transmural nerve stimulation performed by application of square-wave pulses (10 V amplitude, 0.5 ms duration; CRS-ST-04, Experimetria Ltd). The train duration was 60 s followed by a recovery interval of 120 s. Frequency–response relationships with EFS of 1–30 Hz were recorded. In some experiments, frequency–response relationships with EFS (1–30 Hz) were performed in the absence and presence of 10 μM ISO (Sigma, Steinheim, Germany), which was applied 10 min before starting EFS. After four washouts, the same strips were preincubated with or without 100 μM cBIMPS (Biolog, Bremen, Germany) for 15 min, and subsequently frequency–response relationships with EFS were recorded. In order to inhibit PKA, strips were preincubated with 100 μM Rp-cAMPS (Biolog, Bremen, Germany) for 45 min. Data acquisition was performed with the computer-based EXP-D/4 system (Experimetria Ltd). Percentualized EFS curves were calculated with ORIGIN 6.0 (OriginLab Corporation, Northampton, MA, USA).

Western blot analysis of signaling proteins in urinary bladder

Proteins from WT and $BK^{-/-}$ urinary bladder were isolated by homogenization with an Ultra Turrax in buffer (20 mM Tris/HCl, 100 mM NaCl, 2.5 mM dithiothreitol, 2.5 mM EDTA, 2.5 mM benzamidine, 2.5 mM phenylmethanesulfonyl fluoride, 1 $\mu g \cdot \mu L^{-1}$ leupeptin; pH 8.0; 4 °C) followed by centrifugation (17 900 ***g*** 4 °C, 3 min). Protein isolation was always performed in the morning to avoid differences in circadian protein expression. The supernatants were concentrated up to a final volume of ~ 120 μL using a Vivaspin-30 concentrator (Sartorius, Germany). After SDS/PAGE loaded with ~ 120 μg protein per lane, western blot analysis of detrusor smooth muscle proteins was performed with specific primary antibodies (Fig. S2; diluted in 1 × TBST (1% BSA, 0.5% Triton X-100, 0.05 M NaCl/Tris), 5% BSA, 0.05% sodium azide) against PKAα cat [1 : 100], PKA IIα reg (Santa Cruz Biotechnology Inc., Santa Cruz, California, USA; 1 : 100), PKG type 1 ([56] 1 : 300), and a secondary alkaline phosphatase-conjugated donkey anti-(rabbit IgG) (Dianova, Hamburg, Germany; 1 : 5000). For protein quantification, western blots were scanned and signals were quantified using BIODOC analysis software (Biometra, Göttingen, Germany). As internal standard of protein expression, the signal of MAPK (detected with MAPK antibody diluted 1 : 500; Cell Signaling Technology, Danvers, MA, USA) was used.

cAMP measurements in urinary bladder

Dissected urinary bladder was incubated in buffer (120 mM NaCl, 4.5 mM KCl, 1.2 mM $NaH_2PO_4.2H_2O$, 1 mM $MgSO_4$, 1.6 mM $CaCl_2$, 0.0625 mM EDTA, 5.5 mM glucose, 5 mM Hepes, pH 7.4) for 30 min at 37 °C prior to stimulation with or without 10 μM ISO for 1 or 10 min. Then, the tissue was snap-frozen in liquid nitrogen and homogenized in 10% trichloroacetic acid. According to the manufacturer's manual, the resulting supernatant was extracted with water-saturated diethyl ether and assayed for cAMP content using a cAMP EIA system kit (Cayman Chemical, Ann Arbor, MI, USA).

Radiotelemetric analysis of intramural pressure in freely moving mice

An implantable radiotelemetric device (PA-C20; Data Sciences International, St Paul, MN, USA) was used for long-term analysis of intravesical pressure and physical activity in conscious, 4–6-month old WT ($n = 7$) and $BK^{-/-}$ ($n = 8$) mice, which were either litter-matched or age-matched. A conventional isoflurane inhalation regime was used for anesthesia, during which mice were placed upon a heating pad to maintain body temperature. To expose the urinary bladder, a lower midline abdominal incision was made. A 6-0 silk suture was knotted proximal to the border between thick-walled and thin-walled sections of the catheter, and a purse suture was made on the bladder wall. The catheter tip beyond the knot was then inserted into the bladder dome. The sutures were knotted with each other to secure the position of the catheter tip. The transmitter body was placed in the peritoneal cavity. After its fixation, the abdominal incision was closed using nonabsorbable sutures. Inhalation anesthesia was stopped, and mice were transferred to their home cages and kept under infrared light for 2 h. Thereafter, the mice were allowed to recover from the surgical procedure for 7 days. The intramural pressure was continuously recorded (one pressure value every 10 s) from day 7 to day 9 postsurgery. To minimize the influence of the mechanical impact induced by physical activity, it is necessary to analyze intravesical

pressure with respect to the circadian rhythmicity of locomotor activity. The locomotor activity of both genotypes was nearly identical between 8 a.m. and 6 p.m. Intramural pressure values higher than 40 mmHg, which occurred infrequently, were assessed as artefacts caused by movements of the mice transferred to the catheter and were therefore excluded from statistics. Data acquisition was performed using the *dataquest* art data acquisition system (Data Sciences International).

Micturition frequency in freely moving mice

For conditioning, mice were kept in their home cages, which were equipped with a gray-colored paper towel on the bottom. After conditioning on three consecutive days, the micturition frequency was analyzed. Therefore, food and water was removed for 5 h, starting at 9 a.m. Thereafter, 0.3 mL of water was applied though an oral tube, and the mice were brought back to their home cage, equipped with a new gray-colored paper towel. In the following 3 h, the number of micturitions was counted according to the urine spots on the paper towel. This procedure was repeated twice.

Proteomic analysis of the $BK^{-/-}$ urinary bladder

Protein sample preparation—The urinary bladders from six WT and six $BK^{-/-}$ mice were dissected, snap-frozen, and homogenized in DIGE Labelling Buffer (containing 7 M urea, 2 M thiourea, 4% Chaps, 30 mM Tris-base; pH 8.5) using an Ultra Turrax. The tissue preparation was always performed in the morning, to avoid differences in circadian protein expression. After centrifugation (17 900 ***g*** 4 °C, 3 min), each supernatant was concentrated up to a final volume of ~ 100 μL using a Vivaspin-5 concentrator (Vivascience AG, Hannover, Germany), yielding a protein concentration of 5–10 $mg \cdot mL^{-1}$. DIGE labeling and 2D SDS/PAGE was performed with 50 μg of WT and $BK^{-/-}$ protein per gel, as well as with an internal standard containing 50% of all WT samples and 50% of all $BK^{-/-}$ samples. According to the manufacturer's protocol, the WT protein samples were labeled with CyDye Cy3, the $BK^{-/-}$ protein samples with Cy5, and the internal standard with Cy2 (minimal dyes; GE Healthcare Bio-Sciences, Uppsala, Sweden). To minimize differences in protein expression caused by unequal affinity of CyDyes, Cy3 and Cy5 were swapped between WT and $BK^{-/-}$ samples. Labeled WT and $BK^{-/-}$ samples and internal standard were mixed, and the same volume of 2× sample buffer (containing 8 M urea, 130 mM dithiothreitol, 4% Chaps, 2% Pharmalytes 3–10) was added to samples focused on IPG strips (pH 4–7). The residual volume was refilled with rehydration buffer A (8 M urea, 2 M thiourea, 4% Chaps, 65 mM dithiothreitol, 0.7% Pharmalytes 3–10, Bromophenol blue). For focusing samples on IPG strips (pH 6–11), the complete residual volume was refilled with rehydration buffer B (8 M urea, 2 M thiourea, 4% Chaps, 0.7% Pharmalytes 6–11, 1.2% DeStreak, 10% isopropanol, 5% glycerol; Bromophenol blue). For IEF, IPG strips [(pH 4–7) (24 cm, linear; BioRad, Hercules, CA, USA) and (pH 6–11) (18 cm, linear; GE Healthcare)] were used. After IEF, IPG strips were equilibrated for 15 min in buffer A containing 1% dithiothreitol, 6 M urea, 4% SDS, and 0.24 M Tris/HCl, and subsequently for 15 min in buffer B, which had the same composition as buffer A, except that dithiothreitol was replaced by 4.8% iodacetamide. The second dimension of SDS/PAGE was performed on 12% polyacrylamide gels (PROTEAN plus Dodeca Cell; BioRad), which were subsequently scanned on low-fluorescent glass plates using a Typhoon9410 Imager (GE Healthcare). For spot detection and differential

analysis, the software programs decyder 2d 6.5 (GE Healthcare) and proteomweaver (BioRad) were used. The limit for regulation factor was set at 1.3-fold. For spot-picking, silver staining of the gels was performed. Protein spots, which are identified to be regulated in the knockouts, were excised and digested in-gel using trypsin (sequencing grade; Promega, Mannheim, Germany).

NanoHPLC-ESI-MS/MS and database search—The eluted and trypsinized peptide fragments were processed using a Dionex LC Packings HPLC System (Dionex LC Packings, Idstein, Germany). ESI-MS/MS mass spectra were recorded using the high-performance quadrupole time-of-flight (QqToF) mass spectrometer QStar Pulsar I (Applied Biosystems, Applera, Darmstadt, Germany) equipped with a nano-ESI source (ADPC-PRO Column Adapter) and distal coated SilicaTips (FS360-20-10-D-20) (both from New Objective, Woburn, USA). Proteins were identified by correlating the ESI-MS/MS spectra with the NCBI protein sequence database using the mowse algorithm as implemented in the MS analysis software mascot (Matrix Science Ltd, London, UK).

Supplementary Material

Refer to Web version on PubMed Central for supplementary material.

Acknowledgments

We thank C. Kabagema, I. Breuning, S. Leicht, L. Pàsztor, A. Rudzio, S. Wahl and K. Oesterle for excellent technical assistance, O. Planz for generously providing the Typhoon scanner, the Deutsche Forschungsgemeinschaft and SFB773 for financial support, and the Ministerium für Wissenschaft und Kunst in Stuttgart for funding of the Proteom Centrum Tübingen.

Abbreviations

BK	large conductance voltage-dependent and Ca^{2+}-dependent K^+ channel
BK$^{-/-}$	constitutive BK channel knockout
cBIMPS	Sp-5,6-dichloro-1-β-$_D$-ribofuranosylbenzimidazole-3′,5′-monophosphorothioate
Ctr	wild-type littermate control of SM-BK$^{-/-}$ mice
EFS	electrical field stimulation
IbTX	iberiotoxin
ISO	isoproterenol
MAPK	mitogen-activated protein kinase
PKA	protein kinase A (cAMP kinase)
PKG	protein kinase G (cGMP kinase)
PSS	physiological saline solution
Rp-cAMPS	Rp isomer of adenosine-3′,5′-cyclic monophosphorothioate

RyR	ryanodine receptor
SEM	standard error of the mean
SERCA	sarcoendoplasmic reticulum-associated Ca^{2+}-ATPase
SM-BK$^{-/-}$	smooth muscle-specific BK channel knockout
SMMHC	smooth muscle-specific myosin heavy chain
SR	sarcoplasmic reticulum
TEA^{+}	tetraethylammonium
TG2	tissue transglutaminase
UBSMC	urinary bladder smooth muscle cell
UBSM	urinary bladder smooth muscle
WT	wild-type litter mate control of BK$^{-/-}$ mice
β-AR	β-adrenoceptor

References

1. Ouslander JG. Management of overactive bladder. N Engl J Med. 2004; 350:786–799. [PubMed: 14973214]
2. Semins MJ, Chancellor MB. Diagnosis and management of patients with overactive bladder syndrome and abnormal detrusor activity. Nat Clin Pract Urol. 2004; 1:78–84. [PubMed: 16474519]
3. Andersson KE, Wein AJ. Pharmacology of the lower urinary tract: basis for current and future treatments of urinary incontinence. Pharmacol Rev. 2004; 56:581–631. [PubMed: 15602011]
4. Heppner TJ, Bonev AD, Nelson MT. Ca^{2+}-activated K^{+} channels regulate action potential repolarization in rat urinary bladder smooth muscle. Am J Physiol Cell Physiol. 1997; 273:C110–C117.
5. Meredith AL, Thorneloe KS, Werner ME, Nelson MT, Aldrich RW. Overactive bladder and incontinence in the absence of the BK large conductance Ca^{2+}-activated K^{+} channel. J Biol Chem. 2004; 279:36746–36752. [PubMed: 15184377]
6. Thornloe KS, Meredith AL, Knorn AM, Aldrich RW, Nelson MT. Urodynamic properties and neurotransmitter dependence of urinary bladder contractility in the BK channel deletion model of overactive bladder. Am J Physiol Renal Physiol. 2005; 289:F604–F610. [PubMed: 15827347]
7. Werner ME, Knorn A-M, Meredith AL, Aldrich RW, Nelson MT. Frequency encoding of cholinergicand purinergic-mediated signaling to mouse urinary bladder smooth muscle: modulation by BK channels. Am J Physiol Regul Integr Comp Physiol. 2007; 292:R616–R624. [PubMed: 16931654]
8. Wallner M, Meera P, Ottolia M, Kaczorowski GJ, Latorre R, Garcia ML, Stefani E, Toro L. Characterization of and modulation by a beta-subunit of a human maxi K_{Ca} channel cloned from myometrium. Receptors Channels. 1995; 3:185–199. [PubMed: 8821792]
9. Petkov GV, Bonev AD, Heppner TJ, Brenner R, Aldrich RW, Nelson MT. Beta1-subunit of the Ca^{2+}-activated K^{+} channel regulates contractile activity of mouse urinary bladder smooth muscle. J Physiol. 2001; 537:443–452. [PubMed: 11731577]
10. Sausbier U, Sausbier M, Sailer CA, Arntz C, Knaus H-G, Neuhuber W, Ruth P. Ca^{2+}-activated K^{+} channels of the BK-type in the mouse brain. Histochem Cell Biol. 2005; 125:725–741. [PubMed: 16362320]
11. Patel HJ, Giembycz MA, Keeling JE, Barnes PJ, Belvisi MG. Inhibition of cholinergic neurotransmission in guinea pig trachea by NS1619, a putative activator of large-conductance,

calcium-activated potassium channels. J Pharmacol Exp Ther. 1998; 286:952–958. [PubMed: 9694955]

12. Zhang XF, Gopalakrishnan M, Shieh CC. Modulation of action potential firing by iberiotoxin and NS1619 in rat dorsal root ganglion neurons. Neuroscience. 2003; 122:1003–1011. [PubMed: 14643767]
13. Sausbier M, Zhou XB, Beier C, Sausbier U, Wolpers D, Maget S, Martin C, Dietrich A, Ressmeyer AR, Schlossmann J, et al. Reduced rather than enhanced cholinergic airway constriction in mice with ablation of the large conductance Ca^{2+}-activated K^+ channel. FASEB J. 2007; 21:812–822. [PubMed: 17197382]
14. Andersson KE, Hedlund P. Pharmacologic perspective on the physiology of the lower urinary tract. Urology. 2002; 60:13–20. [PubMed: 12493344]
15. Longhurst PA, Levendusky M. Pharmacological characterization of beta-adrenoceptors mediating relaxation of the rat urinary bladder *in vitro*. Br J Pharmacol. 1999; 127:1744–1750. [PubMed: 10455334]
16. Kawatani M, Whitney T, Booth AM, de Groat WC. Excitatory effect of substance P in parasympathetic ganglia of cat urinary bladder. Am J Physiol. 1989; 257:R1450–R1456. [PubMed: 2481406]
17. Brown SM, Bentcheva-Petkova LM, Liu L, Hristov KL, Chen M, Kellett WF, Meredith AL, Aldrich RW, Nelson MT, Petkov GV. Beta-adrenergic relaxation of mouse urinary bladder smooth muscle in the absence of large-conductance Ca2+-activated K+ channel. Am J Physiol Renal Physiol. 2008; 295:F1149–F1157. [PubMed: 18701628]
18. Sandberg M, Butt E, Nolte C, Fischer L, Halbrugge M, Beltman J, Jahnsen T, Genieser HG, Jastorff B, Walter U. Characterization of Sp-5,6-dichloro-1-beta-d-ribofuranosylbenzimidazole-3′, 5′-monophosphorothioate (Sp-5,6-DCl-cBiMPS) as a potent and specific activator of cyclic-AMP-dependent protein kinase in cell extracts and intact cells. Biochem J. 1991; 279:521–527. [PubMed: 1659381]
19. Yamazaki Y, Takeda H, Akahane M, Igawa Y, Nishizawa O, Ajisawa Y. Species differences in the distribution of beta-adrenoceptor subtypes in bladder smooth muscle. Br J Pharmacol. 1998; 124:593–599. [PubMed: 9647486]
20. Yamaguchi O. Beta3-adrenoceptors in human detrusor muscle. Urology. 2002; 59:25–29. [PubMed: 12007519]
21. Uchida H, Shishido K, Nomiya M, Yamaguchi O. Involvement of cyclic AMP-dependent and -independent mechanisms in the relaxation of rat detrusor muscle via beta-adrenoceptors. Eur J Pharmacol. 2005; 518:195–202. [PubMed: 16054622]
22. van der Loop FT, Schaart G, Timmer ED, Ramaekers FC, van Eys GJ. Smoothelin, a novel cytoskeletal protein specific for smooth muscle cells. J Cell Biol. 1996; 134:401–411. [PubMed: 8707825]
23. Maake C, Landman M, Wang X, Schmid DM, Ziegler U, John H. Expression of smoothelin in the normal and the overactive human bladder. J Urol. 2006; 175:1152–1157. [PubMed: 16469643]
24. Paul RJ, Hardin CD, Raeymaekers L, Wuytack F, Casteels R. Preferential support of Ca^{2+} uptake in smooth muscle plasma membrane vesicles by an endogenous glycolytic cascade. FASEB J. 1989; 3:2298–2301. [PubMed: 2528493]
25. Hardin CD, Raeymaekers L, Paul RJ. Comparison of endogenous and exogenous sources of ATP in fueling Ca^{2+} uptake in smooth muscle plasma membrane vesicles. J Gen Physiol. 1992; 99:21–40. [PubMed: 1311020]
26. Xu KY, Zweier JL, Becker LC. Functional coupling between glycolysis and sarcoplasmic reticulum Ca^{2+} transport. Circ Res. 1995; 77:88–97. [PubMed: 7788886]
27. Petkov GV, Nelson MT. Differential regulation of Ca^{2+}-activated K^+ (BK) channels by beta-adrenoceptors in guinea pig urinary bladder smooth muscle. Am J Physiol Cell Physiol. 2005; 288:C1255–C1263. [PubMed: 15677377]
28. Hristov KL, Cui X, Brown SM, Liu L, Kellett WF, Petkov GV. Stimulation of β3-adrenoceptors relaxes rat urinary bladder smooth muscle via activation of the large conductance Ca^{2+}-activated K^+ (BK) channels. Am J Physiol Cell Physiol. 2008; 295:C1344–C1353. [PubMed: 18799656]

29. Tanaka Y, Horinouchi T, Koike K. New insights into β-adrenoceptors in smooth muscle distribution of receptor subtypes and molecular mechanisms triggering muscle relaxation. Clin Exp Pharmacol Physiol. 2005; 32:503–514. [PubMed: 16026507]
30. de Groat WC. Integrative control of the lower urinary tract: preclinical perspective. Br J Pharmacol. 2006; 147:S25–S40. [PubMed: 16465182]
31. Sausbier M, Arntz C, Bucurenciu I, Zhao H, Zhou X-B, Sausbier U, Feil S, Kamm S, Essin K, Sailer CA, et al. Elevated blood pressure linked to primary hyperaldosteronism and impaired vasodilation in BK channel-deficient mice. Circulation. 2005; 112:60–68. [PubMed: 15867178]
32. Wegener JW, Schulla V, Lee TS, Koller A, Feil S, Feil R, Kleppisch T, Klugbauer N, Moosmang S, Welling A, et al. An essential role of $Cav_{1.2}$ L-type calcium channel for urinary bladder function. FASEB J. 2004; 18:1159–1161. [PubMed: 15132976]
33. Fleischmann BK, Murray RK, Kotlikoff MI. Voltage window for sustained elevation of cytosolic calcium in smooth muscle cells. Proc Natl Acad Sci USA. 1994; 91:11914–11918. [PubMed: 7527547]
34. van Eys GJ, Niessen PM, Rensen SS. Smoothelin in vascular smooth muscle cells. Trends Cardiovasc Med. 2007; 17:26–30. [PubMed: 17210475]
35. Niessen P, Rensen S, van Deursen J, De Man J, De Laet A, Vanderwinden JM, Wedel T, Baker D, Doevendans P, Hofker M, et al. Smoothelin-a is essential for functional intestinal smooth muscle contractility in mice. Gastroenterology. 2005; 129:1592–1601. [PubMed: 16285958]
36. Malmqvist U, Trybus KM, Yagi S, Carmichael J, Fay FS. Slow cycling of unphosphorylated myosin is inhibited by calponin, thus keeping smooth muscle relaxed. Proc Natl Acad Sci USA. 1997; 94:7655–7660. [PubMed: 9207148]
37. Dulhunty A, Gage P, Curtis S, Chelvanayagam G, Board P. The glutathione transferase structural family includes a nuclear chloride channel and a ryanodine receptor calcium release channel modulator. J Biol Chem. 2001; 276:3319–3323. [PubMed: 11035031]
38. Lilley GR, Griffin M, Bonner PL. Assays for the measurement of tissue transglutaminase (type II) mediated protein crosslinking via epsilon-(gamma-glutamyl) lysine and N',N'-bis (gamma-glutamyl) polyamine linkages using biotin labelled casein. J Biochem Biophys Methods. 1997; 34:31–43. [PubMed: 9089382]
39. Jones RA, Nicholas B, Mian S, Davies PJ, Griffin M. Reduced expression of tissue transglutaminase in a human endothelial cell line leads to changes in cell spreading, cell adhesion and reduced polymerisation of fibronectin. J Cell Sci. 1997; 110:2461–2472. [PubMed: 9410884]
40. Zemskov EA, Janiak A, Hang J, Waghray A, Belkin AM. The role of tissue transglutaminase in cell–matrix interactions. Front Biosci. 2006; 11:1057–1076. [PubMed: 16146797]
41. Feng JF, Gray CD, Im MJ. Alpha 1B-adrenoceptor interacts with multiple sites of transglutaminase II: characteristics of the interaction in binding and activation. Biochemistry. 1999; 38:2224–2232. [PubMed: 10026307]
42. Chen S, Lin F, Iismaa S, Lee KN, Birckbichler PJ, Graham RM. Alpha1-adrenergic receptor signaling via G_h is subtype specific and independent of its transglutaminase activity. J Biol Chem. 1996; 271:32385–32391. [PubMed: 8943303]
43. Lee M-Y, Chung S, Bang H-W, Baek KJ, Uhm D-Y. Modulation of large conductance Ca^{2+}-activated K^+ channel by $G\alpha_h$ (transglutaminase II) in the vascular smooth muscle cell. Pflügers Arch Eur J Physiol. 1997; 433:671–673. [PubMed: 9049155]
44. Feng JF, Rhee SG, Im MJ. Evidence that phospholipase δ1 is the effector in the G_h (transglutaminase II)-mediated signaling. J Biol Chem. 1996; 271:16451–16454. [PubMed: 8663582]
45. Baek KJ, Kang SK, Damron DS, Im MJ. Phospholipase $C_{\delta 1}$ is a guanine nucleotide exchanging factor for transglutaminase II ($G\alpha_h$) and promotes α_{1B}-adrenoceptor-mediated GTP binding and intracellular calcium release. J Biol Chem. 2001; 276:5591–5597. [PubMed: 11087745]
46. Chou EC, Capello SA, Levin RM, Longhurst PA. Excitatory alpha1-adrenergic receptors predominate over inhibitory beta-receptors in rabbit dorsal detrusor. J Urol. 2003; 170:2503–2507. [PubMed: 14634460]

47. Capello SA, Chieh-Lung Chou E, Longhurst PA. Regional differences in responses of rabbit detrusor to electrical and adrenergic stimulation: influence of outlet obstruction. BJU Int. 2005; 95:157–162. [PubMed: 15638915]
48. Andersson KE. Advances in the pharmacological control of the bladder. Exp Physiol. 1999; 84:195–213. [PubMed: 10081718]
49. Tanaka N, Tamai T, Mukaiyama H, Hirabayashi A, Muranaka H, Ishikawa T, Kobayashi J, Akahane S, Akahane M. Relationship between stereochemistry and the beta3-adrenoceptor agonistic activity of 4′-hydroxynorephedrine derivative as an agent for treatment of frequent urination and urinary incontinence. J Med Chem. 2003; 46:105–112. [PubMed: 12502364]
50. Hewawasam P, Erway M, Thalody G, Weiner H, Bois-sard CG, Gribkoff VK, Meanwell NA, Lodge N, Starrett JE Jr. The synthesis and structure–activity relationships of 1,3-diaryl-1,2,4-(4H)-triazol-5-ones: a new class of calcium-dependent, large conductance, potassium (maxi-K) channel opener targeted for urge urinary incontinence. Bioorg Med Chem Lett. 2002; 12:1117–1120. [PubMed: 11909730]
51. Turner SC, Carroll WA, White TK, Gopalakrishnan M, Coghlan MJ, Shieh CC, Zhang XF, Parihar AS, Buckner SA, Milicic I, et al. The discovery of a new class of large-conductance Ca^{2+}-activated K^+ channel opener targeted for overactive bladder: synthesis and structure–activity relationships of 2-amino-4-azaindoles. Bioorg Med Chem Lett. 2003; 13:2003–2007. [PubMed: 12781183]
52. Du W, Bautista JF, Yang H, Diez-Sampedro A, You SA, Wang L, Kotagal P, Lüders HO, Shi J, Cui J, et al. Calcium-sensitive potassium channelopathy in human epilepsy and paroxysmal movement disorder. Nat Genet. 2005; 37:733–738. [PubMed: 15937479]
53. Christ GJ, Day NS, Day M, Santizo C, Zhao W, Sclafani T, Zinman J, Hsieh K, Venkateswarlu K, Valcic M, et al. Bladder injection of ‘naked’ hSlo/pcDNA3 ameliorates detrusor hyperactivity in obstructed rats *in vivo*. Am J Physiol Regul Integr Comp Physiol. 2001; 281:R1699–R1709. [PubMed: 11641143]
54. Sausbier M, Hu H, Arntz C, Feil S, Kamm S, Adelsberger H, Sausbier U, Sailer CA, Feil R, Hofmann F. Cerebellar ataxia and Purkinje cell dysfunction caused by Ca^{2+}-activated K^+ channel deficiency. Proc Natl Acad Sci USA. 2004; 101:9474–9478. [PubMed: 15194823]
55. Wirth A, Benyó Z, Lukasova M, Leutgeb B, Wettschureck N, Gorbey S, Orsy P, Horváth B, Maser-Gluth C, Greiner E, et al. $G_{(12)}$-$G_{(13)}$-LARG-mediated signaling in vascular smooth muscle is required for salt-induced hypertension. Nat Med. 2008; 14:64–68. [PubMed: 18084302]
56. Pfeifer A, Klatt P, Massberg S, Ny L, Sausbier M, Hirneiss C, Wang GX, Korth M, Aszódi A, Andersson KE, et al. Defective smooth muscle regulation in cGMP kinase I-deficient mice. EMBO J. 1998; 17:3045–3051. [PubMed: 9606187]

Europe PMC Funders Author Manuscripts

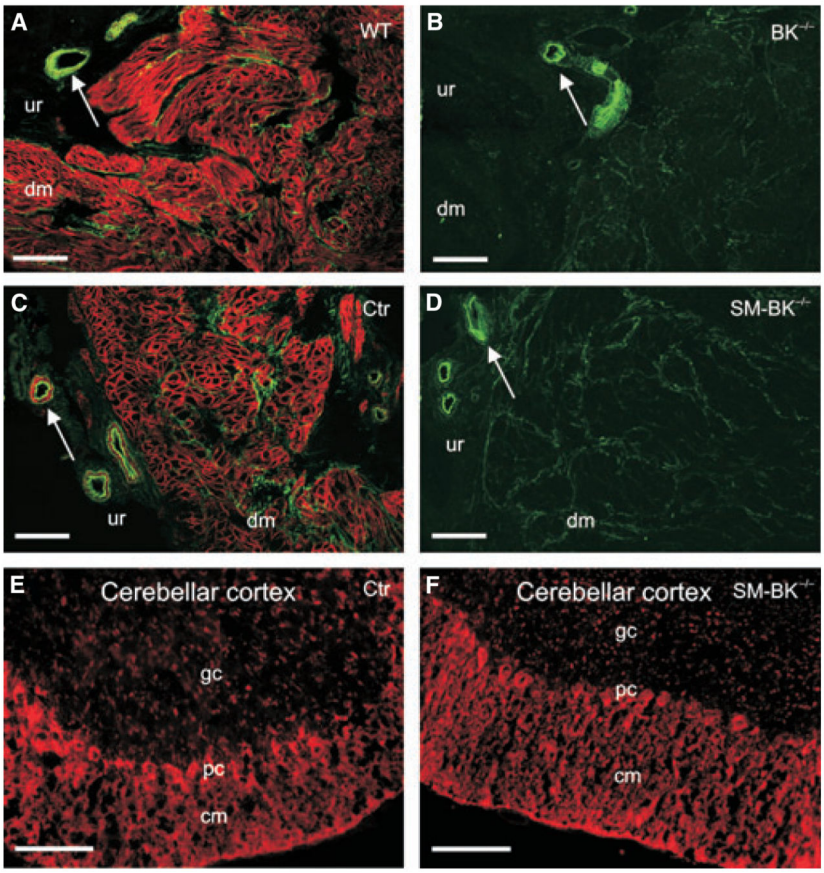

Fig. 1.

Constitutive ($BK^{-/-}$) and temporally controlled smooth muscle-specific ($SMBK^{-/-}$) BK channel ablation. (A–D) Representative sections of detrusor muscle show BK channel immunostaining in the plasma membrane of UBSMCs of WT (A) and Ctr (C) mice. No BK channel staining was observed in $BK^{-/-}$ (B) and SM-$BK^{-/-}$ (D) sections 1 week after tamoxifen application. Note the green autofluorescence of urinary bladder non-smooth muscle cells; arrows indicate blood vessels that are devoid of BK channel immunostaining in $BK^{-/-}$ and SM-$BK^{-/-}$ mice. dm, detrusor muscle; ur, urothelium. (E, F) No change in expression of neuronal BK channels was observed at 2 weeks after tamoxifen application. Ctr cerebellar cortex (E) and SM-$BK^{-/-}$ cerebellar cortex (F) are presented with molecular layer (cm), purkinje cell layer (pc) and granule cell layer (gc). Bars (A–F): 100 μm.

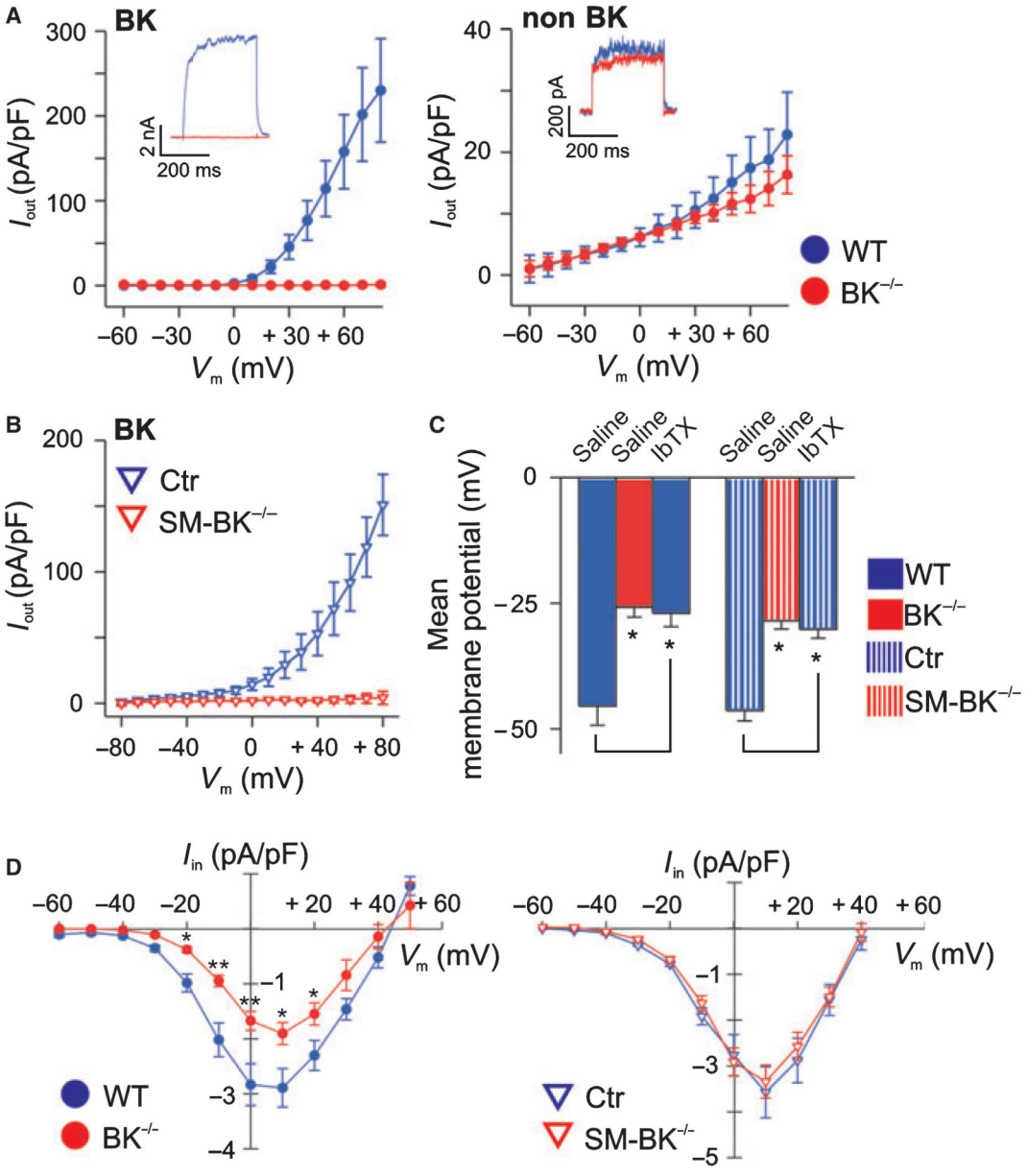

Fig. 2.

(A) Current–voltage relationships of K^+ outward currents from six WT and five $BK^{-/-}$ UBSMCs derived from three urinary bladders of each genotype. Whole cell recordings representing the IbTX-sensitive (left) and IbTX-insensitive (non-BK currents) (right) components of outward currents. The pipette solution contained 300 nM $[Ca^{2+}]_i$ and the holding potential was −10 mV. (B) Current–voltage relationships of K^+ outward currents from nine Ctr and nine SM-$BK^{-/-}$ UBSMCs. (C) Statistics of membrane potential recordings from $BK^{-/-}$ and SM-$BK^{-/-}$ as well as WT and Ctr UBSMCs ± 300 nM IbTX (n = 6–10 cells per genotype). (D) Reduced amplitudes of voltage-gated Ca^{2+} channel currents in $BK^{-/-}$ but not in SM-$BK^{-/-}$ UBSMCs. Peak inward currents were measured in the whole cell patch-clamp configuration, using Ba^{2+} as charge carrier, and are presented as current–

voltage relationships (n = 12 from seven WT mice and n = 14 from six $BK^{-/-}$ mice, as well as n = 10 from four Ctr mice and n = 6 from four SM-$BK^{-/-}$ mice). Voltage-gated Ca^{2+} channel currents were evoked by step depolarizations (300 ms duration) from a holding potential of −60 to +50 mV in 10 mV increments, and current densities are plotted against the respective test potential. Data are means ± standard error of the mean (SEM); *P < 0.05; **P < 0.01.

Europe PMC Funders Author Manuscripts

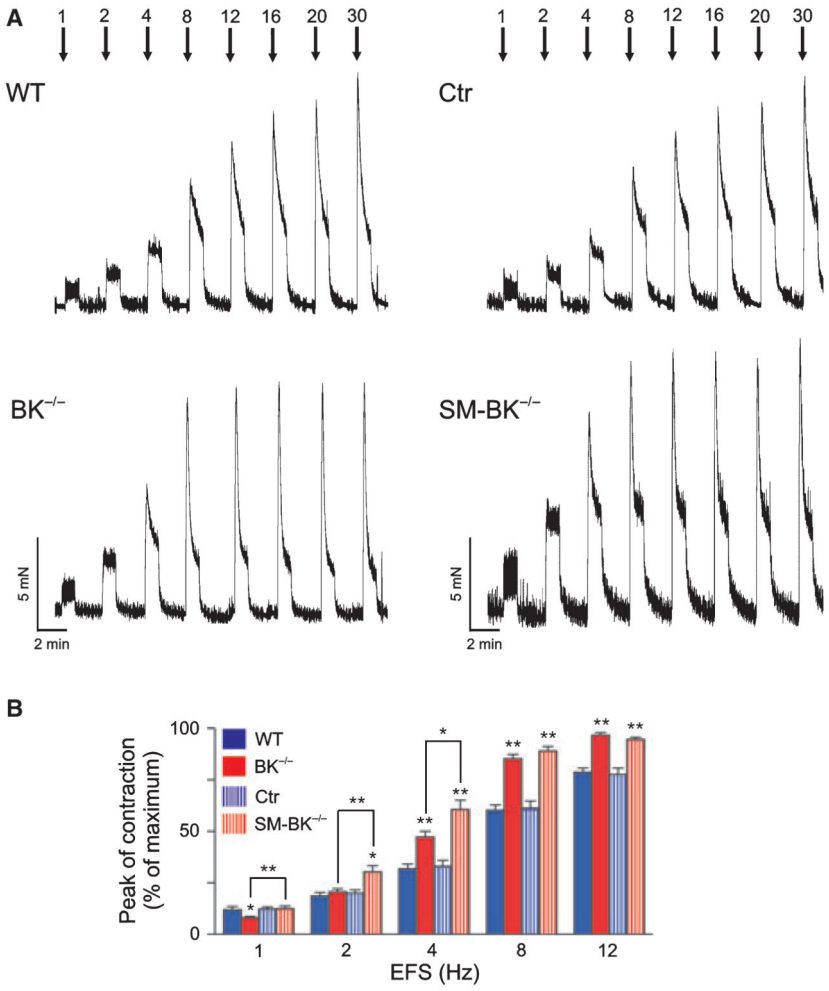

Fig. 3.

EFS-induced contractions of SMBK$^{-/-}$ detrusor muscle are increased as compared to those of BK$^{-/-}$ detrusor muscle. (A) Representative original traces from WT and BK$^{-/-}$ (left panel) as well as Ctr and SM-BK$^{-/-}$ (right panel) detrusor muscle strips showing initial peak contraction followed by tonic contraction in response to EFS at frequencies of 1–30 Hz. (B) Statistics of peak contractions of detrusor muscle strips (WT, 18; BK$^{-/-}$, 20; Ctr, 22; SMBK$^{-/-}$, 21; n = 6–8 mice per genotype). Contractions were normalized to their maxima recorded at 30 Hz. WT/BK$^{-/-}$ and Ctr/SM-BK$^{-/-}$ mice (always F2 generation on an SV129 × C57Bl6 hybrid background) were of equivalent ages and were studied on the same occasion. All data are means ± SEM; *P < 0.05; **P < 0.01.

Europe PMC Funders Author Manuscripts

Europe PMC Funders Author Manuscripts

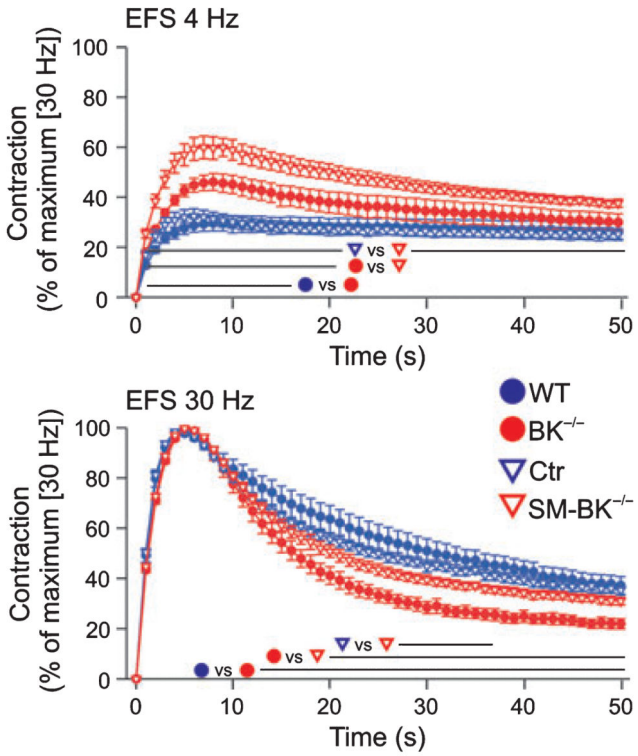

Fig. 4.

Altered contractility kinetics in $BK^{-/-}$ urinary bladder strips during EFS. Time-dependent contraction curves of 18 WT, 20 $BK^{-/-}$, 22 Ctr and 21 SM-$BK^{-/-}$ detrusor strips during EFS at 4 and 30 Hz. Contraction force was referred to maximum contraction at 30 Hz. Note that the absolute values of contractile force at 30 Hz were not statistically different between all genotypes; n = 6–8 mice per genotype. All values are means ± SEM; lines indicate where data points are significantly different ($P < 0.05$).

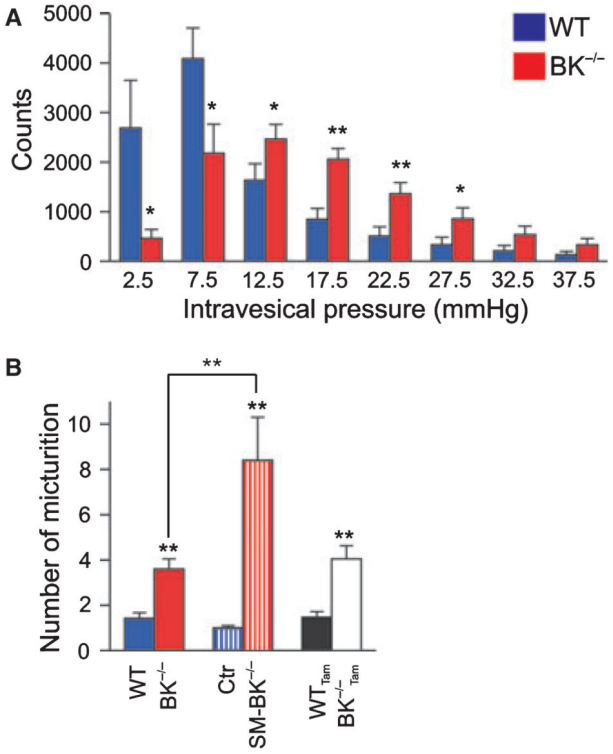

Fig. 5.

Increased intramural pressure and micturition frequency in SM-BK$^{-/-}$ versus BK$^{-/-}$ mice. (A) Statistics of intramural pressures telemetrically recorded from seven WT and eight BK$^{-/-}$ mice. On three consecutive days (days 7–9 after implantation of the telemetric device), the intramural pressure was analyzed every 10 s between 8 a.m. and 6 p.m., the period when WT and BK$^{-/-}$ mice exhibited similar locomotor activity. Each count represents the pressure value of a 10 s interval. Distribution of pressure values in 5 mmHg ranges are presented. The mean pressure of each range is indicated. Movement artefacts were excluded (see also Experimental procedures). (B) Micturition frequency in response to forced water ingestion was analyzed in four WT, five BK$^{-/-}$, six Ctr and six SM-BK$^{-/-}$ mice. To evaluate a putative effect of tamoxifen on micturition frequency, we analyzed also six WT and six BK$^{-/-}$ mice subjected to tamoxifen. The number of micturitions for the 3 h period after water application is given. All data are means ± SEM; *$P < 0.05$; **$P < 0.01$.

Europe PMC Funders Author Manuscripts

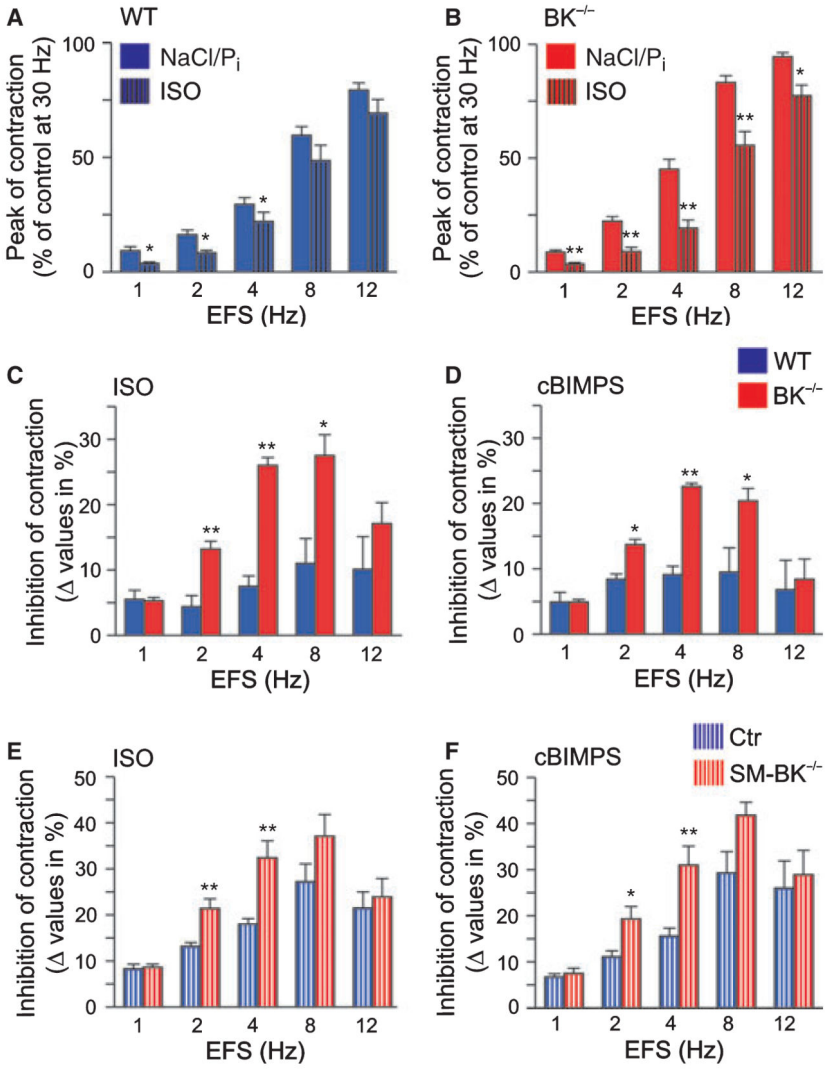

Fig. 6.

Enhanced β-AR/cAMP-mediated inhibition of contractile responses of $BK^{-/-}$ urinary bladder strips. (A, B) Statistics of EFS-induced contractions of WT (A) and $BK^{-/-}$ (B) strips in the absence and presence of 10 μM ISO. Strips were preincubated with either buffer ($NaCl/P_i$) or 10 μM ISO for 10 min prior to EFS. (C) Statistics of ISO-mediated alterations in peak contraction of WT and $BK^{-/-}$ detrusor strips after preincubation with 10 μM ISO for 10 min prior to EFS. (D) Statistical analysis of cBIMPS-mediated reduction of WT and $BK^{-/-}$ detrusor muscle contraction after preincubation with 100 μM cBIMPS for 15 min prior to EFS. (E) Statistics of ISO-mediated alterations in peak contraction of Ctr and SM-$BK^{-/-}$ detrusor muscle strips after preincubation with 10 μM ISO for 10 min prior to EFS. (F) Statistical analysis of cBIMPS-mediated reduction of Ctr and SM-$BK^{-/-}$ detrusor muscle contraction after preincubation with 100 μM cBIMPS for 15 min prior to EFS. All data are means ± SEM; $n = 15$ detrusor muscle strips of four or five mice per genotype; $^{*}P < 0.05$; $^{**}P < 0.01$.

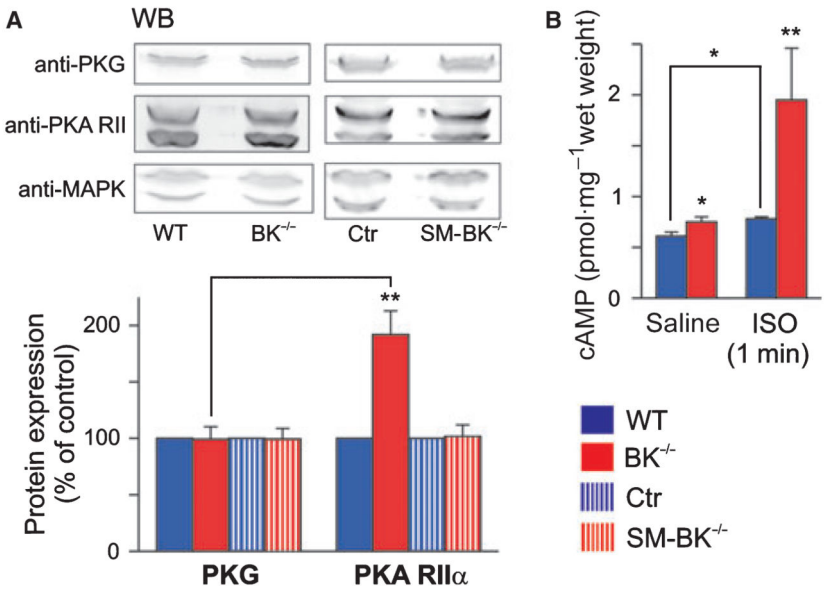

Fig. 7.

Increased cAMP/PKA signaling in $BK^{-/-}$ but not in SM-$BK^{-/-}$ urinary bladder. (A) Representative western blots (WB) of PKA and PKG protein expression, and corresponding statistics in $BK^{-/-}$ and SM-$BK^{-/-}$ urinary bladder as compared to WT or control mice. Expression of PKG and the regulatory (PKA RIIα) subunit of PKA was studied using specific antibodies (for specificity, see also Fig. S2). The WT level was set to 100%. The loading control was MAPK 42/44, which was also the reference for calculation. For statistical significance, PKG expression was used as the reference. (B) cAMP levels under basal conditions (saline) and after incubation with 10 μM ISO for 1 min. All values are means ± SEM; $n = 5$ per genotype; *$P < 0.05$; **$P < 0.01$.

Europe PMC Funders Author Manuscripts

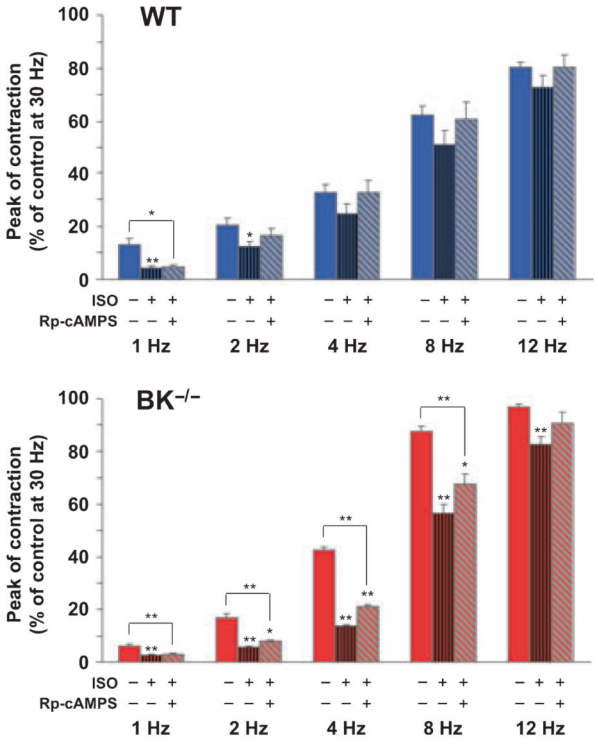

Fig. 8.

Enhanced ISO-mediated inhibition of EFS-induced contractions in $BK^{-/-}$ detrusor muscle strips is only partially reversed by the PKA inhibitor Rp-cAMPS. Statistics of EFS-induced contractions of WT and $BK^{-/-}$ strips (15 detrusor strips from four mice per genotype) preincubated either with 10 μM ISO for 10 min or with 100 μM Rp-cAMPS for 45 min and 10 μM ISO for 10 min prior to EFS. All data are means ± SEM; $*P < 0.05$; $**P < 0.01$.

Europe PMC Funders Author Manuscripts

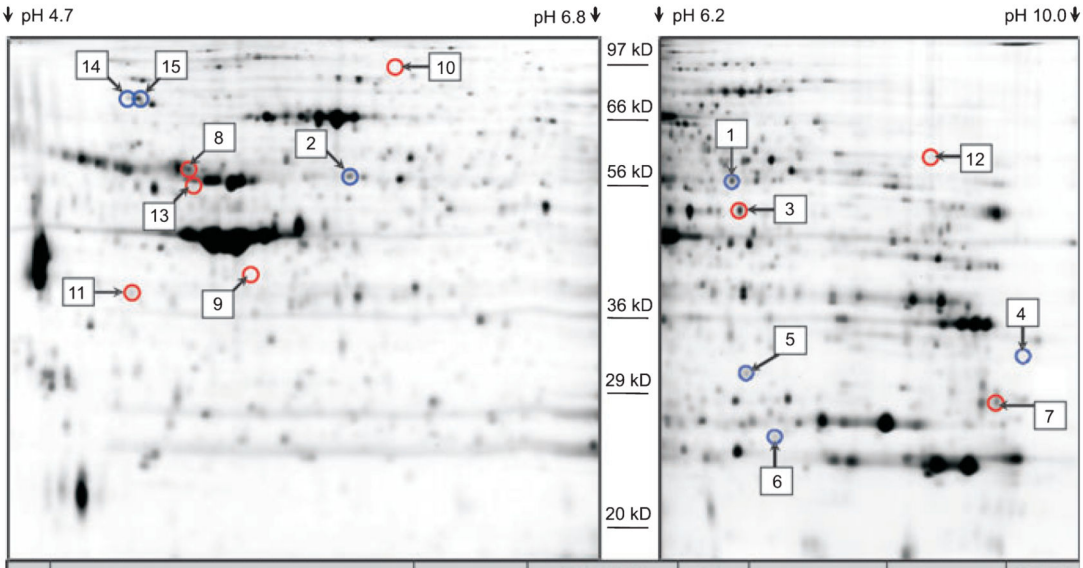

nr.	protein	NCBInr	% protein compared to wt	p-value	calc. MW / pI	det. MW / pI	Mascot score
1	Aldehyde - dehydrogenase, dimeric (class 3)	gi|4322112	*59.2 ± 7.2*	0.0005	50.5 / 7.0	56 / 6.8	414.7
2	Endo A' cytokeratin (5'end put.)	gi|309215	*63.7 ± 3.5*	0.0036	53.2 / 5.3	56 / 5.9	957.5
3	Enolase 3 (beta, muscle)	gi|71059715	**216.4 ± 60.6**	0.0106	47.0 / 6.3	50 / 6.9	597.2
4	Four and a half LIM domains 1	gi|21411428	*71.9 ± 1.9*	0.0024	31.9 / 10.0	32 / 9.5	205.6
5	Glutathione S-transferase omega 1	gi|55154387	*73.0 ± 3.6*	0.0097	27.5 / 6.9	31 / 7.0	131.2
6	Glutathione S-transferase theta 1	gi|31982317	*57.5 ± 2.5*	0.0000	27.4 / 7.9	26 / 7.2	198.6
7	h1-calponin beta	gi|1069993	**199.0 ± 25.0**	0.0011	29.1 / 9.2	29 / 9.2	303.9
8	Polymerase I and transcript release factor	gi|18140061	**140.0 ± 6.0**	0.0000	43.9 / 5.3	59 / 5.3	668.0
9	Protein kinase C delta binding protein	gi|16307146	**150.0 ± 10.3**	0.0002	27.9 / 5.5	40 / 5.5	270.6
10	Similar to protein phosphatase 1, regulatory subunit 12 C, isoform 2	gi|82902895	**188.0 ± 19.8**	0.0000	84.8 / 5.7	96 / 6.0	84.1
11	Small glutamine-rich tetratricopeptide repeat containing protein, alpha	gi|13277936	**136.0 ± 8.5**	0.0014	34.5 / 5.0	38 / 5.1	74.0
12	Smoothelin small isoform S2 (smoothelin A)	gi|7547259	**158.6 ± 7.6**	0.0083	51.6 / 9.6	61 / 8.7	130.5
13	Unnamed protein product (desmin)	gi|74203430	**149.0 ± 13.3**	0.0005	53.5 / 5.2	54 / 5.3	570.8
14	Unnamed protein product (transglutaminase 2, C polypeptide)	gi|26354542	*62.9 ± 5.1*	0.0000	77.0 / 4.9	77 / 5.1	624.9
15	Unnamed protein product (transglutaminase 2, C polypeptide)	gi|26354542	*67.6 ± 3.1*	0.0000	77.0 / 4.9	77 / 5.1	858.7

Fig. 9.

Proteomic adaptation in the $BK^{-/-}$ urinary bladder. Upper: Representative 2D SDS/PAGE gels showing protein-spot localization of regulated urinary bladder proteins (pH range: 4.7–10.0). Fifty micrograms of WT and $BK^{-/-}$ protein and internal standard, fluorescence-labeled with DIGE CyDyes, was applied per gel. Numbers indicate position of protein; red circles indicate upregulated spots, blue circles indicate downregulated spots. Lower: summary of proteome analysis in the $BK^{-/-}$ urinary bladder (bold, upregulation; italic,

downregulation). calc. MW, calculated M_r, including only amino acids; det. MW, detected M_r; pI, isoelectric point; Mascot score, measurement for reliability of MS analysis.

Europe PMC Funders Author Manuscripts

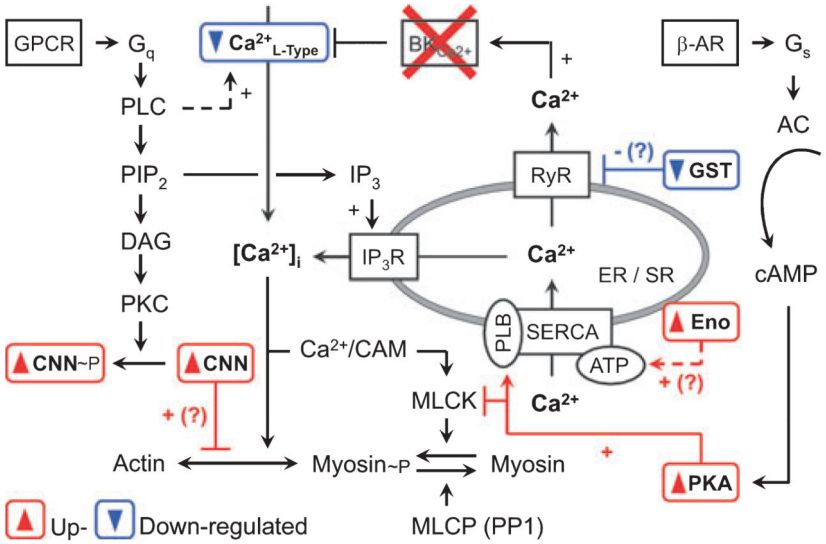

Fig. 10.

Hypothetical network of proteins found in proteome analysis. Note that (?) suggests a putative compensatory mechanism, which might be operative in the $BK^{-/-}$ urinary bladder (for further information see also Results and Discussion). AC, adenylate cyclase; CAM, calmodulin; CNN, calponin h1; DAG, diacylglycerol; Eno, enolase 3; ER, endoplasmic reticulum; GPCR, G-protein-coupled receptor; GST, glutathione S-transferase; IP_3, inositol 1,4,5-trisphosphate; IP_3-R, IP_3 receptor; MLCK, myosin light chain kinase; MLCP, myosin light chain phosphatase; PKC, protein kinase C; PIP_2, phosphatidylinositol 4,5-bisphosphate; PLB, phospholamban; PLC, phospholipase C.

Europe PMC Funders Author Manuscripts